

IONIZED GAS IN THE INNER GALAXY: THE 3 KILOPARSEC ARM

J. C. CERSOSIMO¹

Instituto Argentino de Radioastronomía; and Arecibo Observatory²

Received 1989 October 2; accepted 1989 December 13

ABSTRACT

We report new detections of the H166 α recombination line at high velocity in four directions of the inner Galaxy located at galactocentric distance $R_G < 4$ kpc. Using the present data, along with those published by Lockman at 1.4 GHz and by Caswell and Haynes at 5 GHz, we analyze the distribution of the ionized gas in the inner galaxy. As a result we find that low-density ionized gas is located along the 3 kpc arm. The presence of this gas argues that the H II region are in a latest stage of development. Almost always, the dense H II regions observed at 5 GHz by Caswell *et al.* do not show emission of the H166 α line indicating that these H II regions are in an earliest phase of development.

Subject headings: galaxies: structure — galaxies: The Galaxy — nebulae: H II regions — radio sources: lines

I. INTRODUCTION

The search of H166 α RRL with single dish antennas allows the study of the large scale structure of the ionized hydrogen in a late stage of evolution of the H II region. H I observations in the inner Galaxy showed the relevant feature known as *3 kpc arm*, which is an arc extending from $l = 360^\circ$, $V = -50$ km s⁻¹ to $l = 336^\circ$, $V = -130$ km s⁻¹ located at galactocentric distance³ between 1.7 and 3.4 kpc. Lockman (1980, 1981) did not find evidence for the occurrence of H II regions in the inner arm suggesting that there is very little ionized hydrogen interior to this, except in the immediate vicinity between the 3 kpc arm and the nucleus, where a group of H II regions and type I OH masers form a tilted arc at least 2 kpc long at a distance of ~ 2.7 kpc from the Galactic center.

In this paper we extend the observations of the H166 α line Southern survey (Cersosimo *et al.* 1989) made with the 30 m IAR radio telescope. The new observations have an integration time of 10 hr for each position. The half-power beamwidth of the telescope at 1.42 GHz is 34', the main beam efficiency is ~ 0.87 , and the aperture efficiency is 0.6. In Figure 1 the profiles are presented, the rms noise is ~ 3 mK. The velocity resolution was 15.9 km s⁻¹. The data reduction techniques have been described earlier (Cersosimo *et al.* 1989). The spectra were taken between 345° – 349° along the Galactic plane. We can see significative detection at $V \sim -100$ km s⁻¹ in direction of $l = 345^\circ.5$, 347° , and 348° . The detections at $V \sim 0$ km s⁻¹ in five of the six profiles of Figure 1 show the material associated to the Sagittarius-Carina arm, while the detection around $V \sim -100$ km s⁻¹, kinematically, is located in the inner zone of the galaxy at distances $R_G < 3.4$ kpc. In the direction of $l = 347^\circ.6$ $b = +0^\circ.20$ we observed a known H II region with a spectral resolution of 10 kHz (~ 2 km s⁻¹). The observations and reduction technique have been described by Cersosimo and Loiseau (1984). In Figure 2 is shown the profile obtained, the rms noise is ~ 7 mK.

¹ Fellow of the Consejo Nacional de Investigaciones Científicas y Técnicas (CONICET) of Argentina. Visiting astronomer at Arecibo Observatory.

² The Arecibo Observatory is part of the National Astronomy and Ionosphere Center, which is operated by Cornell University, under a management agreement with the National Science Foundation.

³ For kinematics distances we adopt the resolution of IAU Commission 33 (Burton 1988).

II. DISCUSSION

a) Weak Emission, H166 α

As is shown by the observations the H166 α emission is a good tracer of O associations and open clusters in early evolutionary stages (Hart and Pedlar 1976; Cersosimo 1982). The observations of radio recombination lines (RRL) allow to know the radial velocities and hence kinematic distances of H II regions can be derived. The RRL can usually be characterized as Gaussian profiles. The results of Figures 1 and 2 are summarized in Table 1 where we include the observations detected at high velocity in the fourth quadrant at longitude 350° , 352° , and 356° (Lockman 1980), and the emission at 338.5 (Cersosimo 1990). Col. (1) gives the Galactic longitude. Col. (2) gives the line antenna temperature of the peak. Col. (3) gives the width and col. (4) gives the central radial velocity. The data of Table 1 are displayed with filled circles in the (V, l) -plane of Figure 3. Excluding the source at $l = 347^\circ.6$, the average line temperature of the profiles is ~ 15 mK. Assuming that the emission detected at H166 α line came from low-density gas, it shows that the diffuse gas is located in the locus of the 3 kpc arm, and is well-correlated with the CO emission (Dame *et al.* 1987) between $l \geq 336^\circ$ and 360° . Discussions about the CO feature for $l \geq 350^\circ$ are given by Bania (1977, 1980, 1986). The H166 α emission is not continuous along the length of the arm, and shows isolated clumps of diffuse ionized gas. Let us consider a classical model of low-density H II regions, with $T_e = 5000$ K and a departure from LTE of 20%. The emission measure obtained is low, we obtain $E \sim 400$ pc cm⁻⁶ assuming arbitrarily $\Omega_s/\Omega_A = 1$ where Ω_s and Ω_A are the solid angle of the source and of the antenna, respectively (this mean clumps with diameter ~ 60 pc and electron density ~ 3 cm⁻³). Generally the ionized gas does not appear as an important component of the 3 kpc arm. An explanation has been given by Lockman (1980) indicating that the increased abundance of supernova remnants, energetic particles, and other sources of ionization toward the inner Galaxy has not greatly affected the overall hydrogen ionization rate. The weak high-velocity emission at $338^\circ.5$, located in the inner zone $R_G < 4$ kpc, is at $l \leq 20^\circ$ from the Galactic center, and it appears to merge gradually with the terminal velocity ridge of H I (Kerr, Bowers, and Henderson 1981) around 340° in the confusion zone defined by Caswell and Haynes (1987).

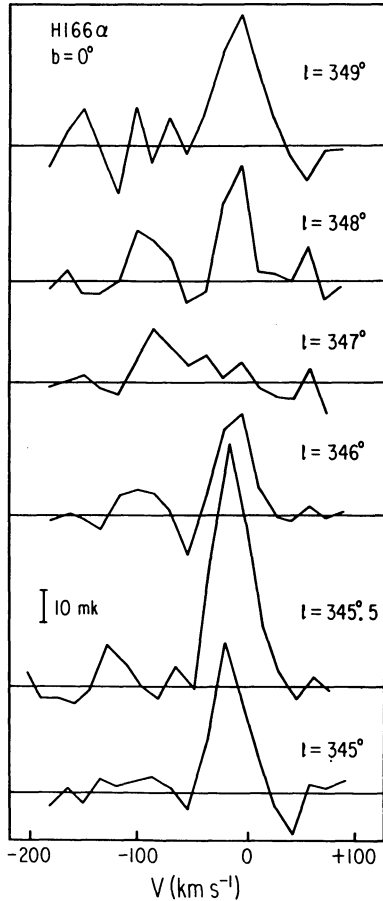


FIG. 1.—The six H166 α spectra taken between 345° and 340° longitude along $b = 0$. The vertical scale is antenna temperature, the horizontal scale is LSR velocity. The spectral resolution is 15.9 km s^{-1} . The longitude of observation is written beside each spectrum.

Barcia *et al.* (1985) show the low-frequency RRL arise in optically thin ionized gas which hardly contributes to the 5 GHz radio continuum emission. On the other hand, Burton and Gordon (1978) and Cersosimo *et al.* (1989) show spatial correlation between H166 α line emission and continuum

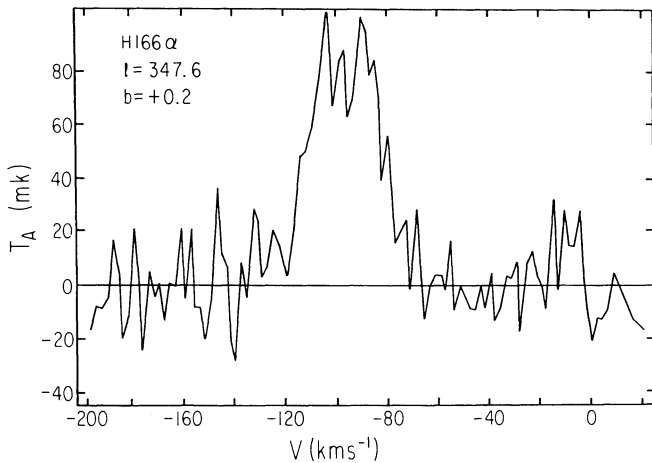


FIG. 2.—Same as in Fig. 1 taken at $l = 347.6$, $b = +0.2$ and with a spectral resolution of 2 km s^{-1} . The strongest line around -90 km s^{-1} came from gas located in the 3 kpc arm. The signal between -20 and 0 km s^{-1} correspond to gas located in the Sagittarius-Carina arm.

TABLE 1
PARAMETERS OF THE H166 α LINE EMISSION ALONG $b = 0$

Galactic Longitude (degree)	Line Temperature (mK)	Line Width (km s^{-1})	Radial Velocity (km s^{-1})
338.5	38	20 ± 8	-112 ± 9
345.5	11	22 ± 10	-120 ± 9
347.0	14	32 ± 12	-85 ± 9
347.6	100	32 ± 2	-98 ± 10
348.0	13	36 ± 12	-100
350.0*	≤ 15	...	-110
352.0*	≤ 15	...	-90
356.0*	≤ 15	...	-80

* Lockman 1980.

source at 5 GHz. This continuum source has been observed at RRL by several authors (Reifestein *et al.* 1970; Caswell and Haynes 1987), the similar velocities of H166 α and H109–110 α lines suggest that the high- and low-density gas must be physically associated (Cersosimo 1990). In order to study the properties of the weak emission in the inner Galaxy we select from the survey of Caswell and Haynes (1987) the H II regions located at galactocentric distances between 1.7–3.4 kpc, their parameters are listed in Table 2. Cols. (1)–(2) show the Galactic coordinates. Col. (3) shows the radial velocity of the 5 GHz RRL (Caswell and Haynes 1987). Col. (4) shows the galactocentric distance, and col. (5) contains the ionizing photons. The asterisks indicate the regions which belong to the tilted arc and with a “G” we indicate the giant H II regions defined by Mezger (1970).

The regions of Table 2 are displayed in the longitude-velocity domain of Figure 3 with filled and open triangles. The main characteristic shown in Figure 3 is that the weak line emission at 1.4 GHz is located into the band of the 3 kpc arm,

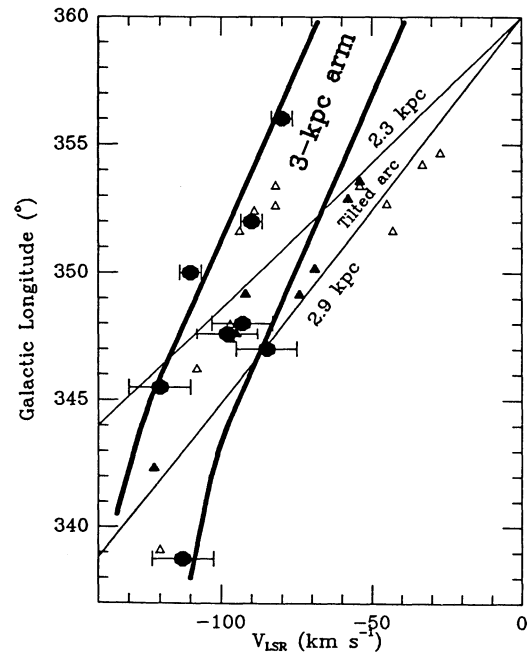


FIG. 3.—H166 α line emitting regions (filled circles) and dense H II regions (triangles) in the inner region of the Galaxy ($R_G \leq 3.7 \text{ kpc}$) between 338° and 360° longitude. The locus of the 3 kpc arm and of the tilted arc are shown. Filled triangles define the locus of the tilted arc.

TABLE 2
PARAMETERS OF HIGH-DENSITY REGIONS

Coordinates		Radial	Galactocentric	Ionizing	Note
l ($^{\circ}$)	b ($^{\circ}$)	Velocity (km s^{-1})	Distance (kpc)	Photons (10^{-48} s^{-1})	
339.089	-0.216	-120	3.1	16.7	
*342.300	+0.314	-122	2.6	111.1	G
346.206	-0.071	-108	2.4	40.8	G
*347.386	+0.266	-97	2.4	54.0	G
*347.600	+0.211	-96	2.4	131.6	G
347.964	-0.439	-97	2.3	10.4	
*349.111	+0.105	-74	2.6	18.8	
*349.140	-0.020	-92	2.2	...	
*350.129	+0.088	-69	2.6	31.9	
351.601	-0.348	-94	1.8	7.5	G
351.617	+0.171	-43	3.3	62.8	
352.398	-0.057	-89	1.7	26.1	
352.676	+0.148	-45	2.9	1.2	
352.611	-0.172	-82	1.8	15.2	
*352.866	-0.199	-58	2.3	13.9	
353.381	-0.114	-82	1.7	...	
353.381	-0.114	-54	2.3	...	
*353.557	-0.014	-54	2.3	56.3	G
354.200	-0.054	-33	3.1	14.5	
354.664	+0.470	-27	3.3	13.5	

NOTE.—G = giant H II regions defined by Hezger 1970.

and by comparing the positions of the circles and triangles we can see that the behavior of the weak 1.4 GHz RRL is not like that found along the Galactic plane (Burton and Gordon 1978; Cersosimo *et al.* 1989) in the sense that the H166 α line of Table 1 does not have clear association with the dense H II regions.

b) The 3 kpc Arm and the Tilted Arc

Although our intention is not to discuss the tilted arc noticed by Lockman (1981) it is interesting to distinguish in the inner Galaxy between both structures. The sources thought to be part of the tilted arc are marked with asterisks in Table 2, and with filled triangles in the (l , b) plane of Figure 3; the feature is aligned along the locus of 2.6 ± 0.3 kpc from the Galactic center. We included three new regions apparently associated with the group. The source at $l = 352.200$, $b = -0.054$, listed by Lockman (1981) as member of the feature, was excluded because it is not located into the locus of 2.6 ± 0.3 kpc. For the H II regions placed into the locus of the tilted arc of Figure 3, we find an inclination of $2^{\circ}5'$ to a plane through $b = 0^{\circ}$. We note that there are no H166 α line emission associated to the tilted arc, and the 50% of the regions located in the tilted arc are giant H II regions (marked with a "G" in Table 2). All H II regions forming the tilted arc are assumed at near distance (Lockman 1981). The Lyman photon flux of the dense southern H II regions between $R_G = 1.7$ and 3.4 kpc is $N_c \sim 7 \times 10^{50} \text{ s}^{-1}$, which originates for 61% in the tilted arc and for 18% in the 3 kpc arm.

It is known that the mass ratio, M_d/M_H , increases sharply toward the Galactic center. The derived values for the mass ratio, is larger value at smaller R_G , 3×10^{-3} for $R_G > 3.5$ kpc, (Deul 1988) and 0.01 for $R_G < 3.5$ (Savage and Mathis 1979). For nonzero optical depth of the dust within the ionized region, the effective radius of the H II regions is smaller than other one without dust. The radius of the ionized hydrogen shell decrease from 0.81 to 0.25 as the optical thickness of the dust increases from 1 to 20, then the fraction of stellar photons

shortward of the Lyman limit, which are absorbed by H atoms rather than by dust, decreases from 0.53 to 0.016 (Spitzer 1978). In such case the Lyman photon flux derived above could actually be one or two orders of magnitude larger. Then for the inner region we estimate a total $N_c \sim 10^{52} \text{ s}^{-1}$. In order to estimate the star formation rate (SFR), we use the Salpeter's analytical expressions of initial mass functions (IMF) given by Güsten and Mezger (1982). A lower and upper termination of stellar mass spectrum of 0.1 and $60 M_{\odot}$, respectively is adopted. We derive a SFR $\sim 0.04 M_{\odot} \text{ yr}^{-1}$ for the 3 kpc arm, and $0.1 M_{\odot} \text{ yr}^{-1}$ for the tilted arc. They are lower than the local SFR, $\sim 0.3 M_{\odot} \text{ yr}^{-1}$, calculated by Güsten and Mezger (1982).

The giant molecular cloud in the 3 kpc arm seems to be stable against gravitational collapse, on the contrary the tilted arc seems to be more efficient star forming than the 3 kpc arm. The mechanism cloud-cloud collision to form OB stars is consistent with a number of previous observations of OB star formation (Scoville *et al.* 1986). The concentration of giant H II regions in the tilted arc can be a result from the convergence of cloud orbits in the spiral potential minimum associated with the density wave. And its deficiency of gas (H I and CO) probably arose through of star formation which was extremely efficient, and little gas remained after formation, but there is no reason to expect star formation reach maximum efficiency at intermediate region in the disk (2–4 kpc), a rotating disk of stars does not exist within the bulge observed in other galaxies (Kormendy 1977). An optional explanation can be the supernova rate and its subsequent heating which was great enough during an earlier epoch to transmute clouds into wind material.

III. SUMMARY

New detections of diffuse ionized gas in the inner Galaxy between 345° – 350° along the Galactic plane are shown. The emitting gas located in the 3kpc arm, has low-emission measure, and the intensity of the emissions confirms a low-

hydrogen ionization rate noticed by Lockman (1981). The detection of the H166 α line using a low-aperture telescope, indicates the existence of a late phase of development of an H II region. It would be useful to search for more diffuse ionized gas at low-frequencies RRL (less than 1 GHz) to clarify the content of the ionized gas in the 3 kpc arm.

I wish to thank the technical staff of the IAR, the director of the NAIC, M. M. Davis for his hospitality and T. Acevedo for making the figures. I am also grateful to D. Van Buren for valuable comments and suggestions. This paper was prepared at the Arecibo Observatory supported by the CONICET of Argentina.

REFERENCES

- Bania, T. M. 1977, *Ap. J.*, **216**, 381.
 ———. 1980, *Ap. J.*, **242**, 95.
 ———. 1986, *Ap. J.*, **308**, 868.
- Barcia, A., Gómez González, J., Lockman, F. J., and Planesas, P. 1985, *Astr. Ap.*, **147**, 237.
- Burton, W. B., and Gordon, M. A. 1978, *Astr. Ap.*, **63**, 7.
- Burton, W. B. 1988, *Galactic and Extragalactic Radioastronomy*, ed. G. L. Verchuur and K. I. Kellermann (Springer).
- Caswell, J. L., and Haynes, R. F. 1987, *Astr. Ap.*, **171**, 261.
- Cersosimo, J. C. 1982, *Ap. Letters Comm.*, **24**, 157.
 ———. 1990, *Ap. J.*, **349**, 67.
- Cersosimo, J. C., Azcárate, I. N., Hart, L., and Colomb, F. R. 1989, *Astr. Ap.*, **208**, 239.
- Cersosimo, J. C., and Loiseau, N. 1984, *Astr. Ap.*, **133**, 93.
- Dame, T. M., Ungerechts, H., Cohen, R. S., de Geus, E. J., Grenier, I. A., May, J., Murph, D. C., Nyman, L. A., and Thaddeus, P. 1987, *Ap. J.*, **322**, 706.
- Deul, E. R. 1988, PhD. thesis. University of Leiden.
- Güsten, R., and Mezger, P. G. 1982, *Vistas Astr.*, **26**, 159.
- Hart, L., and Pedlar, A. 1976, *M.N.R.A.S.*, **176**, 135.
- Kerr, F. J., Bowers, P. F., and Henderson, P. D. 1981, *Astr. Ap. Suppl.*, **44**, 63.
- Kormendy, J. 1977, *Ap. J.*, **217**, 406.
- Lockman, F. J. 1980, *Ap. J.*, **241**, 200.
 ———. 1981, *Ap. J.*, **245**, 459.
- Mezger, P. G. 1970, *IAU Symposium 38, The Spiral Structure of Our Galaxy*, ed. W. Becker, J. Contopoulos (Dordrecht: Reidel), p. 107.
- Reifstein II, E.C., Wilson, T. L., Burke, B. F., Mezger, P. G., and Altenhoff, W. J. 1970, *Astr. Ap.*, **4**, 357.
- Savage, B. D., and Mathis, J. S. 1979, *Ann. Rev. Astr. Ap.*, **17**, 73.
- Scoville, N. Z., Sanders, D. B., and Clemens, D. P. 1986, *Ap. J. (Letters)*, **310**, L77.

J. C. CERSOSIMO: Arecibo Observatory, P.O. Box 995, Arecibo, PR 00613